because it produces a granuloma resulting from the trauma induced by a laser intense enough to rupture Bruch's membrane located between the RPE and choroid, and represents only classic CNV, which is not a major type of CNV such as occult-dominant CNV in humans. Although the CNV model in this study requires aged animals and several months of light exposure, it more closely resembles the human pathology compared to the laser-induced CNV animal models, which will significantly advance the development of novel treatments for AMD.

Materials and methods

Animals

MCP-1$^{-/-}$ mice backcrossed to a C57BL/6 background were purchased from Jackson Laboratory (Bar Harbor, ME). Ccr2$^{-/-}$ mice with a 129xB6 background were generated as described previously (Boring et al., 1997). Littermates were used as controls in each experiment. All experiments were performed in accordance with the Association for Research in Vision and Ophthalmology Statement for the Use of Animals in Ophthalmic and Vision Research.

Light exposure

Freely moving 2-month-old and 12-month-old C57BL/6 male mice were exposed to a blue light-emitting diode (LED) continuously for 1 week (Moritex, Tokyo, Japan; illuminance: 1000 lux, transmission peak wavelength: 480 nm). For low-level light irradiation, freely moving 6-month-old wild-type, MCP-1$^{-/-}$, and Ccr2$^{-/-}$ mice were exposed to a blue LED every 2 days for 6 months (Moritex; illuminance: 500 lux, transmission peak wavelength: 480 nm, Fig. 1A). They were maintained on a 12-hour:12-hour light-dark cycle with dim overhead fluorescent light in the whole room.

Mass spectrometric analysis of phospholipids

Lipid extracts were re-dissolved in methanol:water (90:10) and liquid chromatography/electrospray ionization tandem mass spectrometry (LC/ESI/MS/MS) performed using a Prodigy ODS C18 column for separation of the lipids and the HPLC solvent system (Waters, Milford, MA). Mass spectrometric analyses were performed using ESI/MS/MS in the positive ion, multiple reaction monitoring (MRM) mode (cone energy 30 V/collision energy 25 eV). The MRM transitions used to detect individual oxidized phospholipids were the mass to

charge ratio (*m/z*) for the molecular cation $[M+H]^+$ and their daughter ion 184, the phosphatidylcholine group. Calibration curves for quantitative analyses of individual oxidized phosphatidylcholine molecular species were constructed by mixing a fixed amount of internal standard (ditetradecyl phosphatidylcholine) into various amounts of authentic oxidized phosphatidylcholine samples (Sun et al., 2006).

Immunohistochemistry

Enucleated mouse eyes were immersed in ice-cold phosphate-buffered 4% paraformaldehyde for 6 hours. Eyes were infiltrated with 30% sucrose and embedded in OCT compound (Sakura Finetechnical Co., Tokyo, Japan). Sections (8 μm) were cut, air-dried for 3 hours, and stored at -80°C. Immunofluorescent staining was performed using standard protocols with digitonin permeabilization. Briefly, sections blocked with 5% normal donkey serum were incubated overnight at 4°C with mouse monoclonal antibody to human oxidized phosphatidylcholine, DLH3 (1:100, provided by Dr. Hiroyuki Itabe (1994)), goat polyclonal antibody to mouse MCP-1 (1:100, R&D Systems, Minneapolis, MN), rat monoclonal antibody to F4/80 (1:100, Serotec), rabbit polyclonal antibody to mouse PEDF (1:100, Santa Cruz Biotechnology, Inc., Santa Cruz, CA) , rabbit polyclonal antibody to mouse VEGF or VEGFR2 (1:100, Abcam, Cambridge, MA) . Slides were washed three times with Tris-buffered saline containing 0.1% Tween 20 and incubated with Alexa Fluor 546–conjugated secondary antibodies or Alexa Fluor 488–conjugated secondary antibodies (Invitrogen, Carlsbad, CA) for 60 min at room temperature.

Competitive ELISA for oxidized phospholipids

Relative amounts of oxidized phospholipids in the retinas were evaluated using a competitive ELISA as described in a previous report (Itabe et al., 1994), which is a modified sandwich ELISA procedure for determining oxidized low density lipoprotein (OxLDL). Briefly, microtiter wells precoated with the monoclonal antibody, DLH3 (5 μg/ml in phosphate-buffered saline [PBS], 100 μl/well) were blocked with 1% bovine serum albumin in 50 mM Tris-buffered saline, pH 8.0. One hundred microliters of a solution of lipids extracted from retinas, which were resuspended in PBS, was placed in each well and left at room temperature for 30 min, followed by the addition of 10 μl OxLDL (1 μg/ml). The OxLDL that remained after washing with Tris-buffered saline containing 0.05% Tween 20 was detected by 100 μl sheep anti-human apoB IgG

(Chemicon, Temecula, CA) and 100 μl alkaline phosphatase-conjugated donkey anti-sheep IgG antibody (Chemicon). Alkaline phosphatase reactivity was measured by incubating 1 mg/ml of p-nitrophenylphosphate at 37°C for the appropriate time intervals. Antigenic activity was expressed as a percentage of inhibition, calculated as (Abs (OxLDL)-Abs (sample + OxLDL)) ×100/ (Abs (OxLDL) - Abs (PBS)).

Lipids

Oxidized phospholipids (ON-PC; 9-oxononanoic acid esters of 2-lyso-phosphatidylcholine [2-lyso-PC]) and phospholipids (PLPC; linoleic acid) were purchased from Avanti Polar Lipids, Inc. (Alabaster, AL)

Cell culture

The human retinal pigment epithelial cell line ARPE-19 was obtained from the American Type Culture Collection and cultured in Dulbecco's modified Eagle's medium/F-12 supplemented with 10% fetal bovine serum, penicillin (100 U/mL), and streptomycin sulfate (100 μg/mL). Cells were grown at 37°C in humidified 5% CO_2 and split twice a week when approximately 90% confluent. Cells were obtained at passage 12 and used at passages 14 to 18. RPE cells were subcultured in 24-well tissue culture plates at a density of $4x10^4$ cells/well. Seven days after reaching confluence, the medium was changed and cells were incubated in serum-free Dulbecco's modified Eagle's medium in the presence or absence of untreated phospholipids or oxidized phospholipids at concentrations of 0, 10, 25, or 50 μg/ml. After 6 h, the medium was collected, filter sterilized, and stored at -80°C until use for ELISA for MCP-1. Each condition was evaluated in triplicate, and results were repeated in at least three independent experiments.

Real-time RT-PCR for MCP-1

For analysis of MCP-1 mRNA levels in the retina-RPE-choroid complex, total RNA was isolated from the respective samples (RNeasy Mini Kit, Qiagen Inc., Valencia, CA) and reverse-transcribed with a cDNA synthesis kit (First-Strand, Amersham Biosciences/GE Lifesciences; Piscataway, NJ). We used β-actin as the invariant control. Commercially available primers and probe sets of the mouse MCP-1 genes (Invitrogen) were prepared for the analysis. We performed amplification, detection, and data analysis using the ABI PRISM 7900 Sequence Detection

System.

ELISA

The retina-RPE-choroid complex was placed into 200 ml of lysis buffer supplemented with protease inhibitors and sonicated. The lysate was centrifuged at 15,000 rpm for 10 min at 4°C. The supernatants and amount of secreted MCP-1,VEGF, or PEDF in the conditioned medium from RPE cells were assayed with ELISA kits for MCP-1,VEGF (R&D Systems) and PEDF (BioVendor, Czech Republic) according to the manufacturer's protocols. Protein concentrations were determined using the BCA protein assay kit (Pierce, Rockford, IL).

Subretinal injection of oxidized phospholipids or non-oxidized phospholipids

Subretinal injections were performed on 8-week old C57BL/6J, $MCP^{-/-}$, and $Ccr2^{-/-}$ mice. The mice received phospholipids (50 μg/ml) in one eye and oxidized phospholipids (50 μg/ml) in the other eye. At this concentration, there was no significant difference in the cell survival of ARPE-19 cells after exposure to oxidized phospholipids and phospholipids. Pulled glass micropipettes were calibrated to deliver 2 μl of vehicle upon depression of a foot switch (FemtoJet Express; Eppendorf). The mice were anesthetized with ketamine hydrochloride (100 mg/kg body weight) and xylazine (10 mg/kg body weight), pupils were dilated with topical 1% tropicamide (Santen Inc., Napa, CA), and the sharpened tip of the micropipette (Eppendorf) was passed through the sclera 1 mm posterior to the limbus and positioned adjacent to the retina. Depression of the foot switch caused the injection fluid to penetrate the retina. Injections were performed using a condensing lens system, which allowed visualization of the retina during the injection. This technique is atraumatic and the direct visualization allows for confirmation of a successful injection by the appearance of a small retinal bleb. All injections were made at a site approximately two-thirds of the distance vertically from the optic disc to the ora serrata in the superior retina.

Histology examination

For histology, the eyes were enucleated and fixed with 4% paraformaldehyde for 1 hour h at 4° . After removing the anterior segment, the eyecups were fixed again in 4% paraformaldehyde overnight, dehydrated in 30% sucrose for 6 hours, and then embedded in Tissue-Tek® OCT

compound. The eyecups were sectioned into 7-μm thick slices and stained with hematoxylin and eosin.

Electron microscopy

The retina-RPE-choroid was fixed in 2.5% glutaraldehyde solution for 2 hours and 1% osmium tetroxide solution for 1 hour, rinsed in PBS, dehydrated in EtOH, and then embedded in epoxy resin (Nissin EM Quetor 812). Thick (1.0 μm) and ultrathin sections (80 nm) were cut on a ultramicrotome (Reichert Ultracut E). The thick sections were stained with toluidine blue and examined by light microscopy. Ultrathin sections were stained with 4% uranyl acetate and lead citrate and then examined with an H-7650 transmission electron microscope (Hitachi, Tokyo, Japan).

Fluorescein Angiography

Fluorescein angiography was recorded using a fundus camera (RC-2, Kowa) with an external 66-diopter condensing lens mounted between the camera and the eye. The pupil was dilated with topical 1% tropicamide (Santen) and mice were injected intraperitoneally with 10% sodium fluorescein (Ak-Fluor) at a dose of 0.03 ml/5 g weight.

PBN Treatment

α-Phenyl-N-tert-butylnitrone (PBN), a commonly used free radical spin trap (Ranchon I., et al. 2003), was purchased from Sigma-Aldrich (St. Louis, MO) and dissolved in saline. PBN (50 mg/kg) was intraperitoneally administered once daily for a week with light irradiation.

MCP-1 siRNA treatment

Transfection of MCP-1 siRNA (Santa Cruz Biotechnology, Inc.) was performed according to the manufacturer's instructions. ARPE-19 cells treated with MCP-1 siRNA were incubated in serum-free Dulbecco's modified Eagle's medium in the presence or absence of untreated phospholipids or oxidized phospholipids at concentrations of 0, 10, 25, or 50 μg/ml. After 6 h, the medium was collected, filter sterilized, and stored at -80°C until use for ELISA for VEGF or PEDF. Each condition was evaluated in triplicate, and the results were repeated in at least three independent experiments.

Statistical Analysis

All data are presented as mean ± s.d. and were compared using the Student's t test. A P value of less than 0.05 was considered statistically significant.

Acknowledgements

We are deeply grateful to the late Professor Yasuo Tano who contributed immeasurably to our study. His memory will live on through our work. We thank Israel F. Charo for providing the CCR2-deficient mice.

References

Age-Related Eye Disease Study Research Group, SanGiovanni, J. P., Chew, E. Y., Clemons, T. E., Ferris, F. L., 3rd, Gensler, G., Lindblad, A. S., Milton, R. C., Seddon, J. M. and Sperduto, R. D. (2007). The relationship of dietary carotenoid and vitamin A, E, and C intake with age-related macular degeneration in a case-control study: AREDS Report No. 22. *Arch. Ophthalmol.* 125, 1225-32.

Ambati, J., Anand, A., Fernandez, S., Sakurai, E., Lynn, B. C., Kuziel, W. A., Rollins, B. J. and Ambati, B. K. (2003). An animal model of age-related macular degeneration in senescent Ccl-2- or Ccr-2-deficient mice. *Nat. Med.* 9, 1390-7.

Baba, T., Bhutto, I. A., Merges, C., Grebe, R., Emmert, D., McLeod, D. S., Armstrong, D. and Lutty, G. A. (2010). A rat model for choroidal neovascularization using subretinal lipid hydroperoxide injection. *Am. J. Pathol.* 176, 3085-97.

Beatty, S., Koh, H., Phil, M., Henson, D. and Boulton, M. (2000). The role of oxidative stress in the pathogenesis of age-related macular degeneration. *Surv. Ophthalmol.* 45, 115-34.

Bochkov, V. N., Philippova, M., Oskolkova, O., Kadl, A., Furnkranz, A., Karabeg, E., Afonyushkin, T., Gruber, F., Breuss, J., Minchenko, A. et al. (2006). Oxidized phospholipids stimulate angiogenesis via autocrine mechanisms, implicating a novel role for lipid oxidation in the evolution of atherosclerotic lesions. *Circ. Res.* 99, 900-8.

Boring, L., Gosling, J., Chensue, S. W., Kunkel, S. L., Farese, R. V., Jr., Broxmeyer, H. E. and Charo, I. F. (1997). Impaired monocyte migration and reduced type 1 (Th1) cytokine responses in C-C chemokine receptor 2 knockout mice. *J. Clin. Invest.* 100, 2552-61.

Clemons, T. E., Milton, R. C., Klein, R., Seddon, J. M. and Ferris, F. L., 3rd. (2005). Risk factors for the incidence of Advanced Age-Related Macular Degeneration in the Age-Related Eye Disease Study (AREDS) AREDS report no. 19. *Ophthalmology* 112, 533-9.

Cruickshanks, K. J., Klein, R. and Klein, B. E. (1993). Sunlight and age-related macular degeneration. The Beaver Dam Eye Study. *Arch. Ophthalmol.* 111, 514-8.

Edwards, A. O., Ritter, R., 3rd, Abel, K. J., Manning, A., Panhuysen, C. and Farrer, L. A. (2005). Complement factor H polymorphism and age-related macular degeneration. *Science* 308, 421-4.

Furnkranz, A., Schober, A., Bochkov, V. N., Bashtrykov, P., Kronke, G., Kadl, A., Binder, B. R., Weber, C. and Leitinger, N. (2005). Oxidized phospholipids trigger atherogenic inflammation in murine arteries. *Arterioscler. Thromb. Vasc. Biol.* 25, 633-8.

Grossniklaus, H. E., Ling, J. X., Wallace, T. M., Dithmar, S., Lawson, D. H., Cohen, C., Elner, V. M., Elner, S. G. and Sternberg, P., Jr. (2002). Macrophage and retinal pigment epithelium expression of angiogenic cytokines in choroidal neovascularization. *Molecular Vision* 8, 119-26.

Haines, J. L., Hauser, M. A., Schmidt, S., Scott, W. K., Olson, L. M., Gallins, P., Spencer, K. L., Kwan, S. Y., Noureddine, M., Gilbert, J. R. et al. (2005). Complement factor H variant increases the risk of age-related macular degeneration. *Science* 308, 419-21.

Hollyfield, J. G., Bonilha, V. L., Rayborn, M. E., Yang, X., Shadrach, K. G., Lu, L., Ufret, R. L., Salomon, R. G. and Perez, V. L. (2008). Oxidative damage-induced inflammation initiates age-related macular degeneration. *Nat. Med.* 14, 194-8.

Itabe, H., Takeshima, E., Iwasaki, H., Kimura, J., Yoshida, Y., Imanaka, T. and Takano, T. (1994).

A monoclonal antibody against oxidized lipoprotein recognizes foam cells in atherosclerotic lesions. Complex formation of oxidized phosphatidylcholines and polypeptides. *J. Biol. Chem.* 269, 15274-9.

Kamei, M., Yoneda, K., Kume, N., Suzuki, M., Itabe, H., Matsuda, K., Shimaoka, T., Minami, M., Yonehara, S., Kita, T. et al. (2007). Scavenger receptors for oxidized lipoprotein in age-related macular degeneration. *Invest. Ophthalmol. Vis. Sci.* 48, 1801-7.

Klein, R. J., Zeiss, C., Chew, E. Y., Tsai, J. Y., Sackler, R. S., Haynes, C., Henning, A. K., SanGiovanni, J. P., Mane, S. M., Mayne, S. T. et al. (2005). Complement factor H polymorphism in age-related macular degeneration. *Science* 308, 385-9.

Lu, B., Rutledge, B. J., Gu, L., Fiorillo, J., Lukacs, N. W., Kunkel, S. L., North, R., Gerard, C. and Rollins, B. J. (1998). Abnormalities in monocyte recruitment and cytokine expression in monocyte chemoattractant protein 1-deficient mice. *J. Exp. Med.* 187, 601-8.

Malek, G., Li, C. M., Guidry, C., Medeiros, N. E. and Curcio, C. A. (2003). Apolipoprotein B in cholesterol-containing drusen and basal deposits of human eyes with age-related maculopathy. *Am. J. Pathol.* 162, 413-25.

Ranchon I., LaVail MM., Kotake Y., Anderson RE. (2003). Free radical trap phenyl-N-tert-butylnitrone protects against light damage but does not rescue P23H and S334ter rhodopsin transgenic rats from inherited retinal degeneration. J Neurosci. 23(14):6050-7.

Sun, M., Finnemann, S. C., Febbraio, M., Shan, L., Annangudi, S. P., Podrez, E. A., Hoppe, G., Darrow, R., Organisciak, D. T., Salomon, R. G. et al. (2006). Light-induced oxidation of photoreceptor outer segment phospholipids generates ligands for CD36-mediated phagocytosis by retinal pigment epithelium: a potential mechanism for modulating outer segment phagocytosis under oxidant stress conditions. *J. Biol. Chem.* 281, 4222-30.

Suzuki, M., Kamei, M., Itabe, H., Yoneda, K., Bando, H., Kume, N. and Tano, Y. (2007).

Oxidized phospholipids in the macula increase with age and in eyes with age-related macular degeneration. *Molecular Vision* 13, 772-8.

Tan, J. S., Wang, J. J., Flood, V., Rochtchina, E., Smith, W. and Mitchell, P. (2008). Dietary antioxidants and the long-term incidence of age-related macular degeneration: the Blue Mountains Eye Study. *Ophthalmology* 115, 334-41.

Taylor, H. R., West, S., Munoz, B., Rosenthal, F. S., Bressler, S. B. and Bressler, N. M. (1992). The long-term effects of visible light on the eye. *Arch. Ophthalmol.* 110, 99-104.

Tsutsumi, C., Sonoda, K. H., Egashira, K., Qiao, H., Hisatomi, T., Nakao, S., Ishibashi, M., Charo, I. F., Sakamoto, T., Murata, T. et al. (2003). The critical role of ocular-infiltrating macrophages in the development of choroidal neovascularization. *J. Leukoc. Biol.* 74, 25-32.

van Leeuwen, R., Boekhoorn, S., Vingerling, J. R., Witteman, J. C., Klaver, C. C., Hofman, A. and de Jong, P. T. (2005). Dietary intake of antioxidants and risk of age-related macular degeneration. *JAMA* 294, 3101-7.

Yamada, K,,Sakurai, E., Itaya, M,,Yamasaki, S., Ogura, Y.(2007). Inhibition of laser-induced choroidal neovascularization by atorvastatin by downregulation of monocyte chemotactic protein-1 synthesis in mice. *Invest Ophthalmol Vis Sci.* 48(4):1839-43.

Yates, J. R., Sepp, T., Matharu, B. K., Khan, J. C., Thurlby, D. A., Shahid, H., Clayton, D. G., Hayward, C., Morgan, J., Wright, A. F. et al. (2007). Complement C3 variant and the risk of age-related macular degeneration. *N. Engl. J. Med.* 357, 553-61.

Zhou, Y., Sheets, K.G., Knott, E.J., Regan C.E. Jr., Tuo, J., Chan, C.C., Gordon, W.C., Bazan, N.G(2011). Cellular and 3D optical coherence tomography assessment during the initiation and progression of retinal degeneration in the Ccl2/Cx3cr1-deficient mouse. *Exp Eye Res.* 93(5):636-48.

Financial Disclosure

M.K. was supported by a Grant-in-Aid for Scientific Research from the Ministry of Education, Science, and Culture of Japan. S.L.H. was supported by NIH grant P01 HL087018-020001.

Competing Interest

The authors have declared that no competing interests exist.

Figure legends

Figure 1. Blue-light irradiation induces phospholipid oxidation in the retina.

(A) Light exposure apparatus. Freely-moving mice were exposed to blue light using an LED with a transmission peak wavelength of 480 nm and an intensity of 1000 lux for the subacute experiments, and 500 lux for the chronic experiments.

(B) Some oxidized phosphatidylcholine species significantly increased in the light-irradiated retinas. Of the linoleic acid esters of 2-lyso-PC, ON-PC significantly increased ($p<0.001$) after light exposure (1000 lux, continuously 1 week). In the docosahexaenoic acid esters of 2-lyso-PC, KOHA-PC and S-PC showed significant increases ($p=0.037$ and 0.006) after light exposure. A-PC, azeleic acid esters of 2-lyso- phosphatidylcholine; ON-PC, 9-oxononanoic acid esters of 2-lyso- phosphatidylcholine; HOHA-PC, 4-hydroxy-7-oxohept-5-enoic acid esters of 2-lyso-phosphatidylcholine; KOHA-PC, 4,7-dioxohept-6-enoic acid esters of 2-lyso-phosphatidylcholine; OB-PC, 4-oxobutyric acid esters of 2-lyso- phosphatidylcholine; S-PC, succinic acid esters of 2-lyso- phosphatidylcholine.

(C-F) Immunohistochemistry for oxidized phospholipids (ON-PC). Oxidized phospholipids (red) are present throughout the sensory retina, RPE, and choroid, and seem more prominent in 12-month-old mice (E) than in 2-month-old mice (C). Light irradiation increased immunostaining in both 2-month-old (D) and 12-month-old (F) mice. Interestingly, oxidized phospholipids in the outer plexiform layer, the photoreceptor outer segments, retinal pigment epithelium (RPE), and choroid were more apparent in the older mice (D) compared with the younger mice (F). Scale bars, 50 μm. GCL, ganglion cell layer; IPL, inner plexiform layer; INL, inner nuclear layer; OPL, outer plexiform layer; ONL, outer nuclear layer; PR, photoreceptor outer segments; RPE, retinal pigment epithelium.

(G) Relative amounts of oxidized phospholipids in the retinas were evaluated with competitive

ELISA. Oxidized phospholipids increased 2.2 and 2.3 folds in the retinas of 2- and 12-month-old irradiated mice, respectively, when compared with non-irradiated mice. There were 1.7 fold more ($p=0.003$) oxidized phospholipids in the 12-month-old irradiated retinas compared with the 2-month-old irradiated retinas. There was no significant difference between 2-month-old and 12-month-old control retinas. 2M, 2-month-old mice; 12M, 12-month old mice. ($n = 10$ mice per group; mean±s.d.) **, $P<0.001$; *, $P=0.003$; n.s., no significance.

Figure 2. Oxidized phospholipids induce monocyte chemoattractant protein-1 (MCP-1) in RPE cells in vitro and light irradiation elicits MCP-1 in the RPE in vivo.

(A) Oxidized phospholipids induce MCP-1 secretion in RPE cells. The ELISA demonstrated that the amounts of MCP-1 protein increased in the supernatants of RPE cells incubated with oxidized phospholipids in a dose-dependent manner (*: $P<0.001$ compared with non-oxidized phospholipids).

(B) Real-time PCR revealed increases of MCP-1 mRNA after light irradiation in vivo. MCP-1 mRNA levels were undetectable in the non-irradiated 2-month-old mice, but in the light-irradiated 2-month-old mice, the MCP-1 mRNA level was 0.51% relative to the β-actin mRNA level. MCP-1 mRNA levels increased in the light-irradiated 12-month-old mice compared to the non-irradiated 12-month-old mice ($n = 6$ mice per group, mean±s.d.). **, $P<0.001$; *, $P=0.003$ compared with non-irradiated mice.

(C) MCP-1 protein also showed a significant increase after light irradiation. In the non-irradiated 2-month-old mice, the MCP-1 protein was undetectable with ELISA, but in the light-irradiated 2-month-old mice, the MCP-1 protein level was 6.62 pg/mg protein. MCP-1 protein levels increased in the 12-month-old light-irradiated mice compared to the non-irradiated 12-month-old mice ($n = 6$ mice per group, mean±s.d.). *, $P<0.001$ compared with non-irradiated mice.

(D) Immunohistochemistry for MCP-1 in the eye with light irradiation. MCP-1 signals (green) are observed in the RPE of 12-month-old light-irradiated mouse retinas. Scale bars, 50 μm. GCL, ganglion cell layer; IPL, inner plexiform layer; INL, inner nuclear layer; OPL, outer plexiform layer; ONL, outer nuclear layer; PR, photoreceptor outer segments; RPE, retinal pigment epithelium.

(E) Light irradiation induced macrophage accumulation in the choroid. The immunoreactivity for F4/80 increased in the choroid of the 12-month-old mice after light irradiation (500 lux) for 2

months (right), while no immunoreactivity were detected in the non-irradiated 12-month-old mice (left). Scale bars, 50 μm.

Figure 3. Oxidized phospholipids induce CNV formation in wild-type mice and no CNV in Ccr2-/- and MCP-/- mice.

Representative photomicrographs of chorioretinal sections from wild-type (A, B), MCP-1-/- (C, D) and Ccr2-/- (E, F) mice at 1 month after subretinal injections of non-oxidized phospholipids (A, C, E) or oxidized phospholipids (B, D, F). CNV (asterisk) was observed only in eyes of wild-type mice with oxidized phospholipid injections (B). Scale bars, 50 μm.

Figure 4. Long-term, low-intensity photic stress induces CNV in wild-type mice, but not in Ccr2-/- and MCP-/- mice.

(A) Electron micrograph showing very mild, subtle sub-RPE deposits (arrowheads) in the non-irradiated wild-type mice, (B) basal laminar deposits (asterisk),an essential histopathologic feature of AMD, in long-term, low-intensity light-irradiated wild-type mice. Vacuoles (arrows) containing membranous material were present on the basal side of RPE. Scale bars, 5 μm.

(C) A fundus photograph of a long-term, low-level light-irradiated mouse retina showed a small, white, round lesion appearing as a CNV.

(D) Fluorescein angiography of the same lesion as (C) showed hyperfluorescence, indicating an occult type CNV.

(E) Histology of the CNV detected in the long-term, low-level light-irradiated wild-type mouse retina. Neovascularization (arrows) from the choroid develops in the subretinal space, which closely resembles CNV, as observed in human AMD. Scale bars, 20 μm.

(F) Macrophages accumulating around the CNV lesion ingest oxidized phospholipids. The electron micrograph shows a macrophage-like cell engulfing the photoreceptor outer segment (asterisk, right: higher magnification). Scale bars, 1 μm. Immunohistochemistry shows that macrophages (green) ingest oxidized phospholipids (red). Scale bar, 10 μm.

(G) Neither MCP-1-/- (n=4) nor Ccr2-/- mice (n=6) showed CNV formation after long-term, low-level light irradiation. CNV also did not develop in any of the control mice in each group. Scale bars, 50 μm.

Figure 5. α-Phenyl-N-tert-butylnitrone (PBN) reduces phospholipids oxidation and monocyte chemoattractant protein-1 (MCP-1) caused by light irradiation

Immunohistochemistry for oxidized phospholipids (red) in 12-month-old mice (A-C). Light irradiation increased immunostaining (B) compared with control mice(A). α-Phenyl-N-tert-butylnitrone (PBN) treatment reduced immunostaining, especially in the ganglion cell layer (GCL), inner nuclear layer (INL), photoreceptor outer segments (PR), retinal pigment epithelium (RPE), and choroid (C). Immunohistochemistry for monocyte chemoattractant protein-1 (MCP-1) (green) in 12-month-old mice (D-F). Light irradiation increased immunostaining (E) compared with control mice(D). PBN treatment reduced immunostaining in INL and RPE (F). Scale bars, 50 μm. GCL, ganglion cell layer; IPL, inner plexiform layer; INL, inner nuclear layer; OPL, outer plexiform layer; ONL, outer nuclear layer; PR, photoreceptor outer segments; RPE, retinal pigment epithelium. (G) Real-time PCR revealed increases in MCP-1 mRNA after light irradiation in vivo with PBN treatment. MCP-1 mRNA levels increased in the light-irradiated mice compared to the non-irradiated mice and decreased in the light-irradiated mice with PBN treatment compared with no-treatment light irradiated mice (n = 6 mice per group, mean±s.d.). *, $P<0.05$.

(H) MCP-1 protein also showed a significant increase after light irradiation and decreased with PBN treatment compared with no-treatment light irradiated mice. (n = 6 mice per group, mean±s.d.). **, $P<0.001$;*, $P=0.022$

Figure 6. VEGF expression in light induced CNV and decrease of VEGF expression by MCP-1 siRNA treatment in RPE cells

(A) Immunoreactivity of VEGF (green) and (B) VEGFR2 (red) expressed in the light-induced CNV lesion. Scale bars, 50 μm. (C) RPE cells released more VEGF with oxidized phospholipid treatment than with non-oxidized phospholipids. VEGF protein levels decreased significantly with MCP-1 siRNA treatment compared with non- treatment**, $P<0.001$; *, $P<0.05$.(D) PEDF immunoreactivity was weak in the light-induced CNV lesion. Scale bar, 50 μm.(E) PEDF protein levels did not change significantly in RPE cells following treatment with oxidized phospholipids or non-oxidized phospholipids. The PEDF protein levels were not affected by MCP-1 siRNA.

Figure 1

A

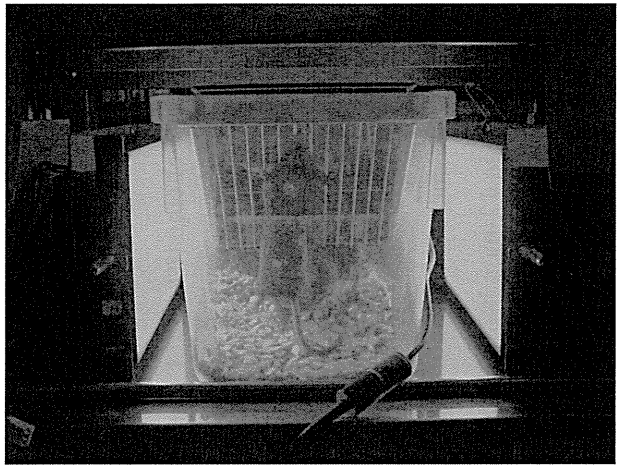

B

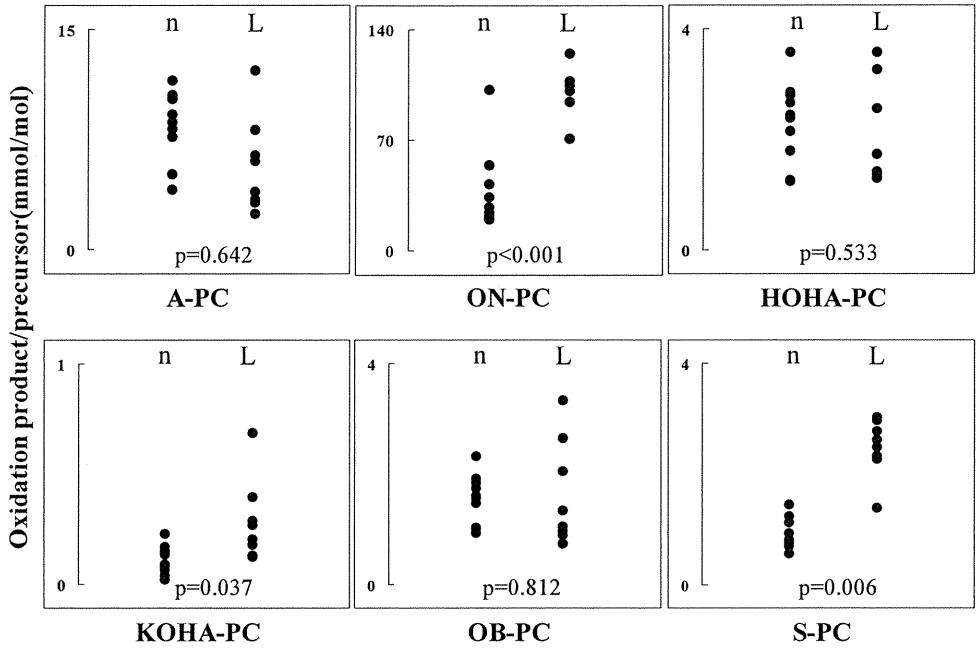

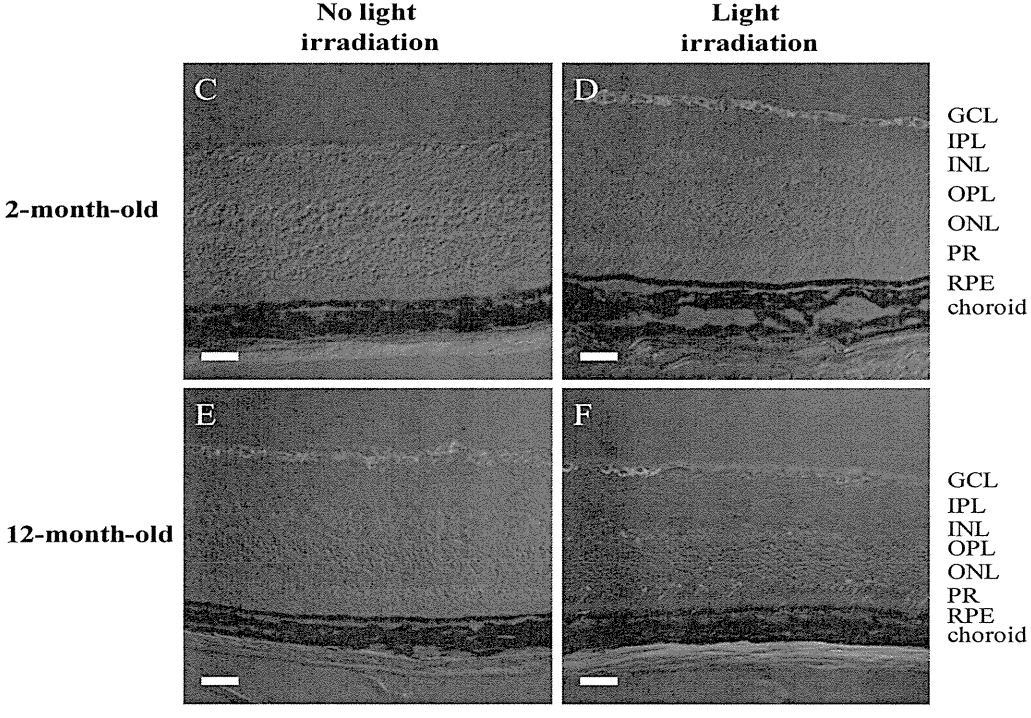

G

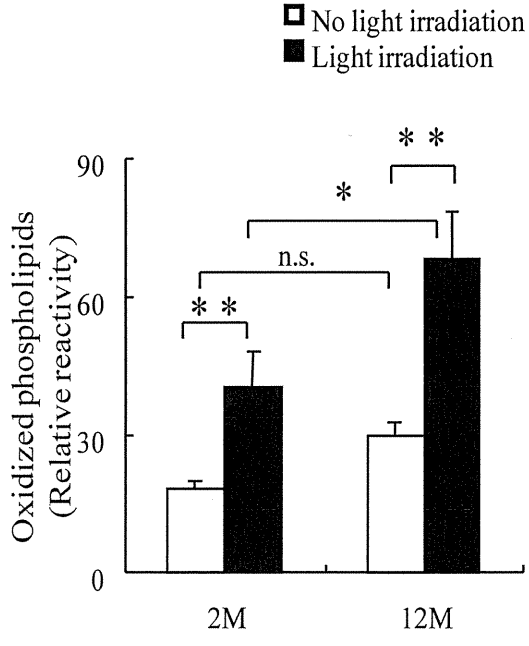

Figure 2

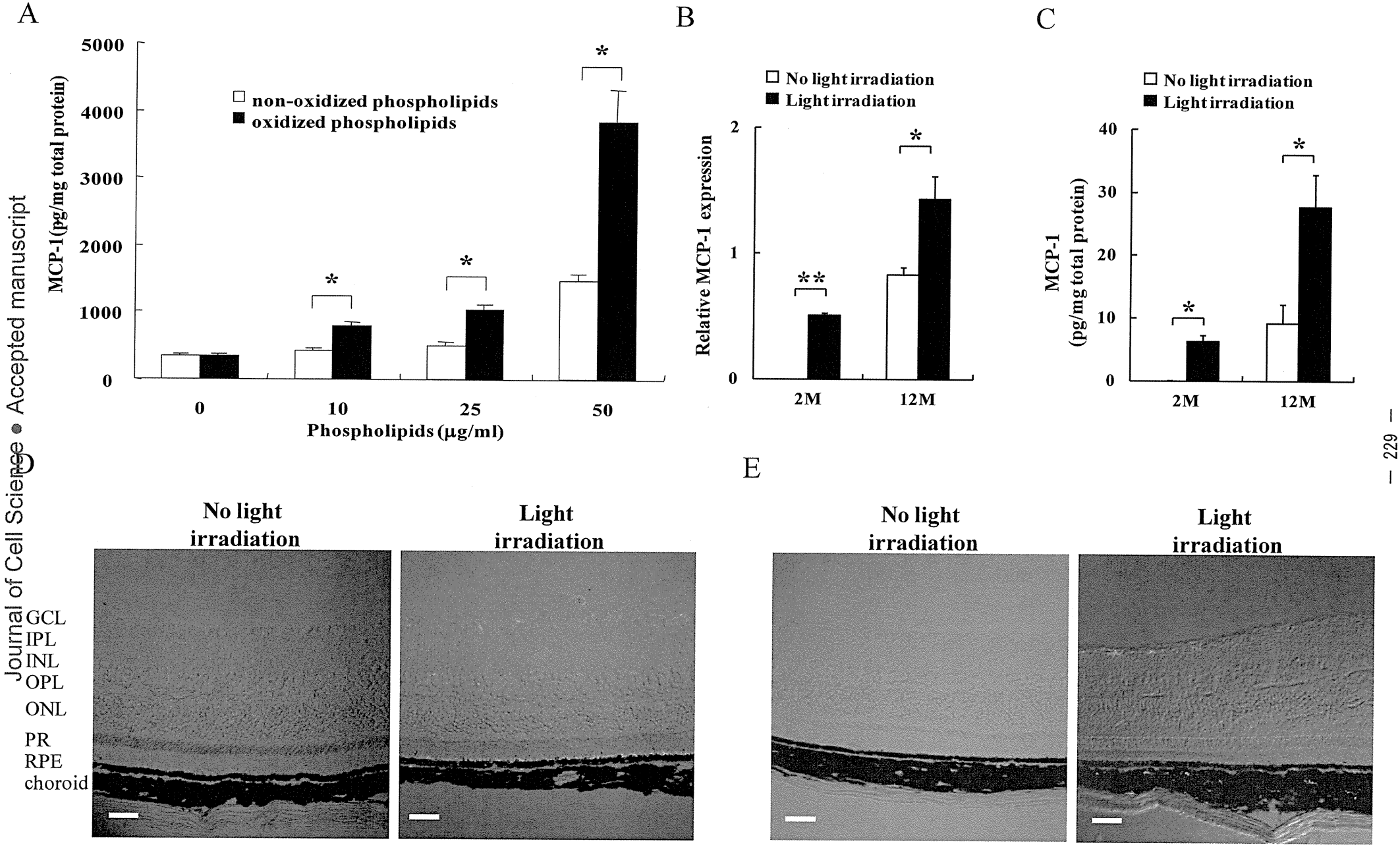

Figure 3

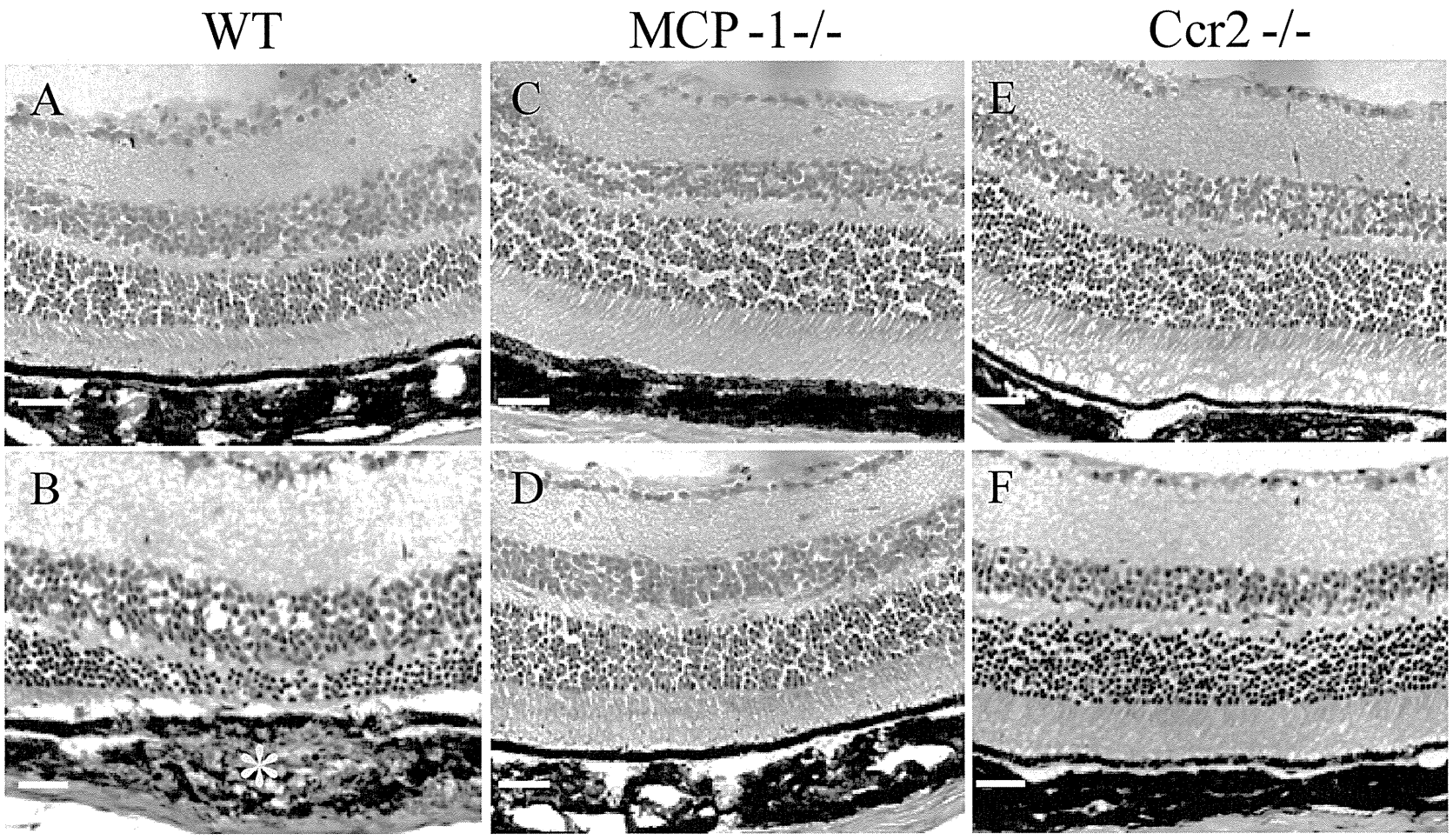

Figure 4

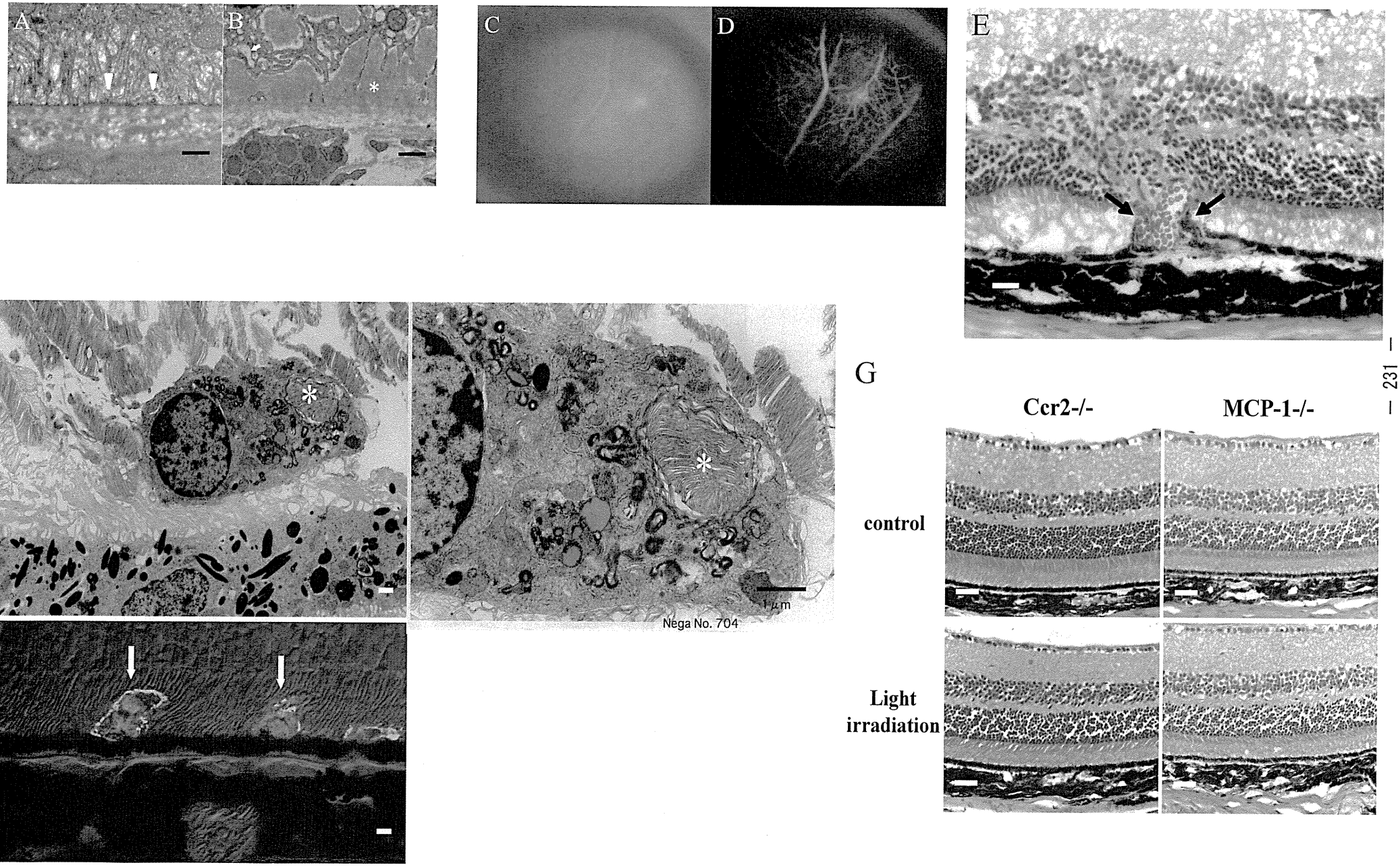

Figure 5

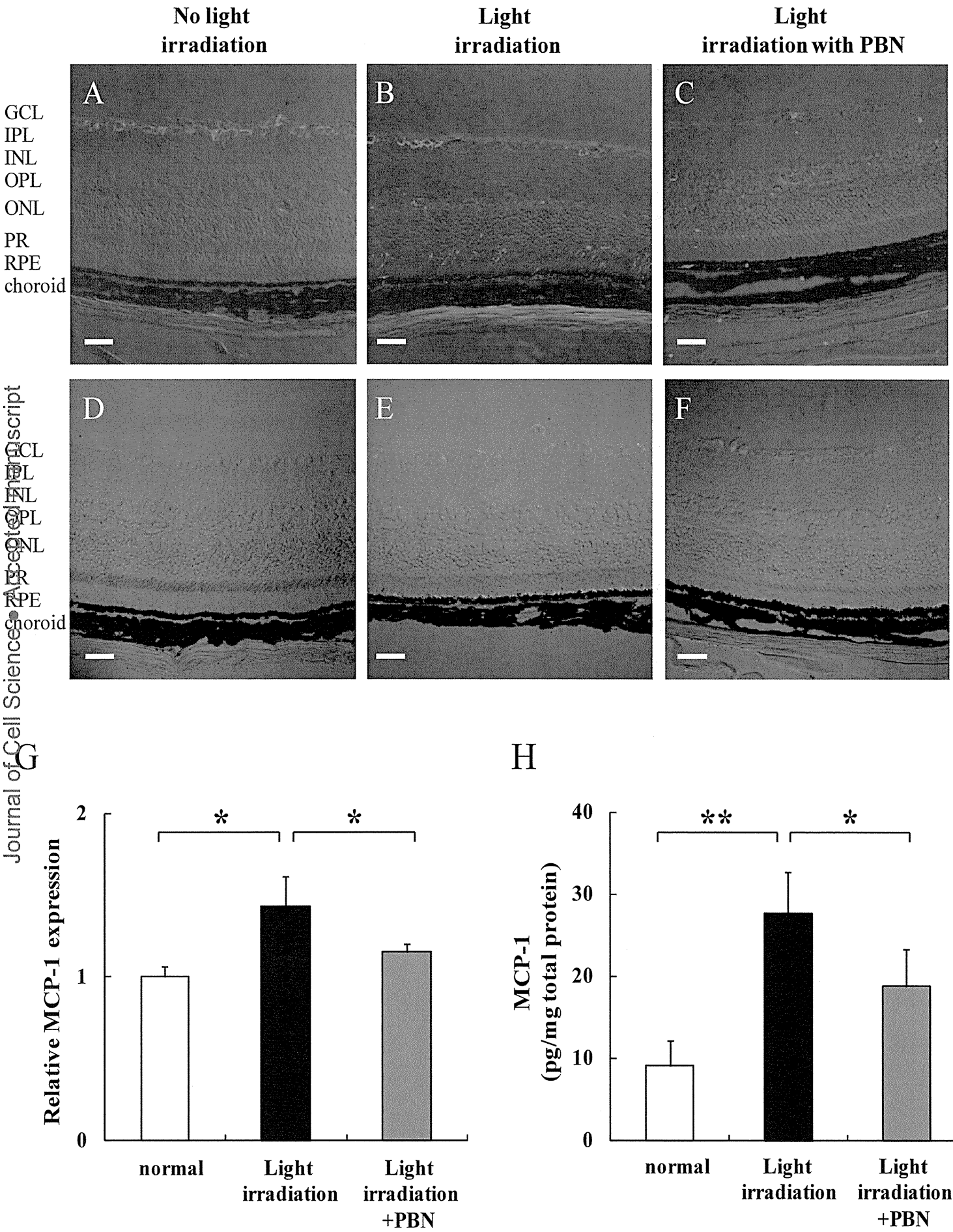

Figure 6

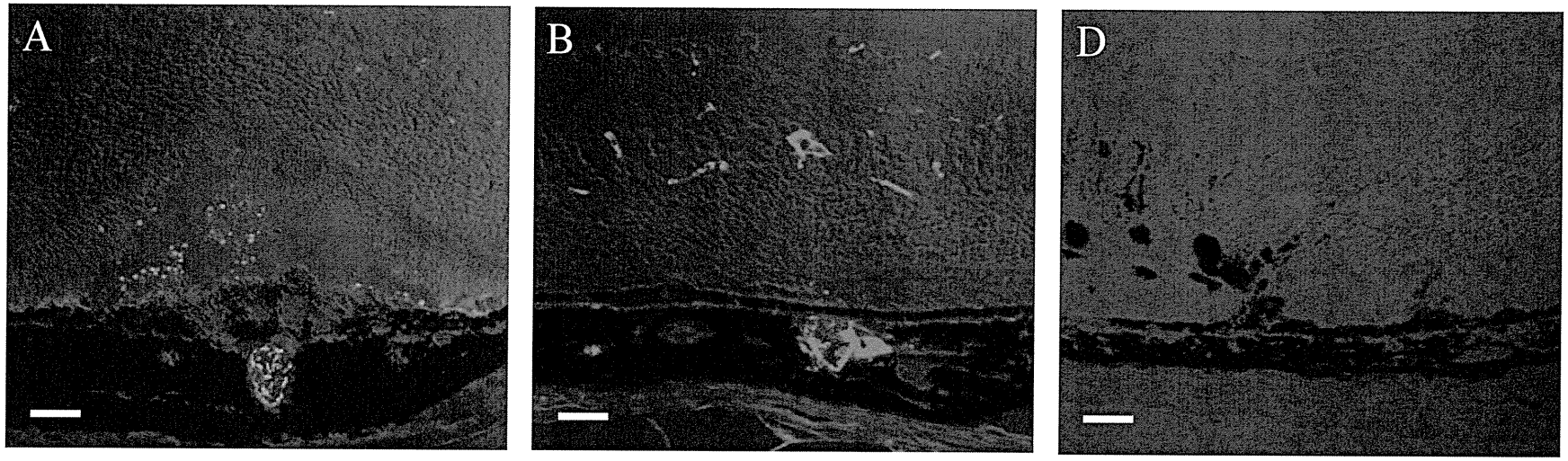

C

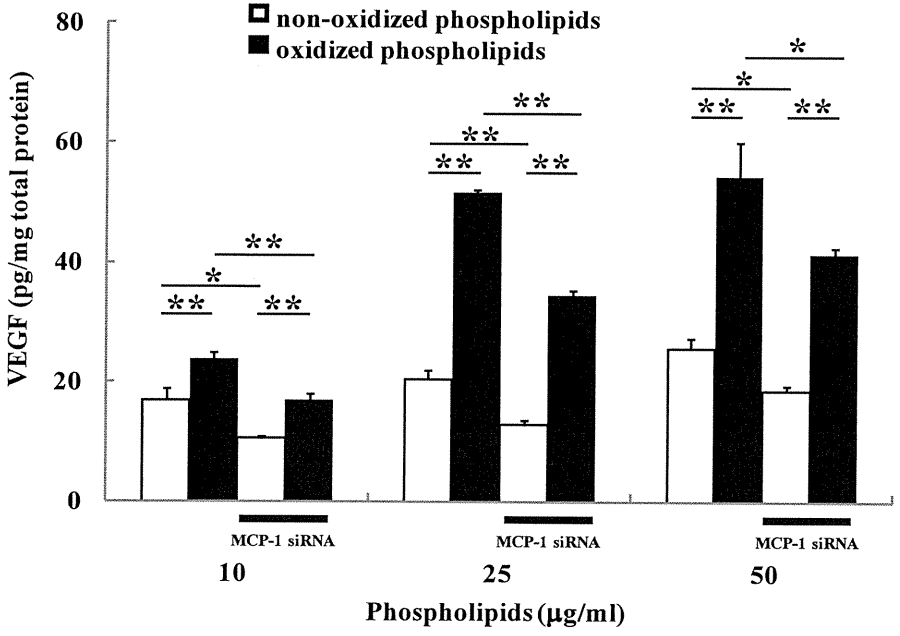

E